Controlled particle generation in an inductively coupled plasma

M. Schulze, A. von Keudell, and P. Awakowicz

Citation: Applied Physics Letters 88, 141503 (2006); doi: 10.1063/1.2193041
View online: http://dx.doi.org/10.1063/1.2193041
View Table of Contents: http://scitation.aip.org/content/aip/journal/apl/88/14?ver=pdfcov
Published by the AIP Publishing

Controlled particle generation in an inductively coupled plasma

M. Schulze[a] and A. von Keudell
Arbeitsgruppe Reaktive Plasmen, Ruhr-Universität Bochum, Universitätsstrasse 150, 44780 Bochum, Germany

P. Awakowicz
Lehrstuhl für Allgemeine Elektrotechnik und Plasmatechnik, Ruhr-Universität Bochum, Universitätsstrasse 150, 44780 Bochum, Germany

(Received 16 December 2005; accepted 22 February 2006; published online 6 April 2006)

By injecting pulses of acetylene into an inductive argon/helium discharge, carbon clusters with diameters in the range of 10–50 nm are produced. These particles cause an instability of the plasma, which becomes visible as an oscillation of the emission intensity. The particles are analyzed *ex situ* using atomic force microscopy and scanning electron micrographs. A unique linear dependence between particle size and oscillation time period is found. Thereby the oscillation phenomenon can serve as monitor signal to control the size of plasma produced particles. © *2006 American Institute of Physics*. [DOI: 10.1063/1.2193041]

In the past decade, dust formation in reactive plasmas has been investigated for many applications.[1,2] This research began with the need to reduce particle formation in processing plasmas used in the semiconductor industry. In the meantime, also beneficial applications of particles have been established. In particular, small particles with diameters below 10 nm can serve as quantum dots in electronic circuits or as photonic devices. Embedded in an amorphous matrix, nanoparticles can induce photoluminescence[3,4] or they can enhance the electronic properties of silicon thin film solar cells.[5]

The adjustment of the particle diameter is often performed empirically by varying the growth time in the plasma. The *in situ* characterization of the properties of very small particles, however, is an unresolved issue. Optical methods such as laser scattering cannot be applied for particles with a diameter below $d \simeq 20$ nm, because the cross section for light scattering scales with d^6. Current methods to control particle growth in rf driven plasmas work indirectly by exploiting the feedback between particles and plasma performance. A typical example are *V-I* probes that measure the spectrum of the rf current to the powered electrode. The formation of particles in a plasma causes its impedance to change, which becomes apparent in the intensity of the harmonics of the driving frequency.[6] However, since the intensity of the harmonics is influenced by the whole rf circuitry, a frequent recalibration of the feedback is necessary.

In Ref. 7, a different method has been proposed to monitor particle properties: an instability is triggered by injecting particles in an inductive plasma, which becomes visible as an oscillation of the plasma emission. It has been postulated that a periodic movement of the particles within the plasma leads to fluctuations in the plasma heating efficiency. The resulting modulation of the plasma emission can easily be detected by a photodiode. In this letter the frequency of the observed plasma oscillations is correlated with the particle diameter. It will be shown that the oscillation time period uniquely depends on the particle diameter and can serve as a monitor signal to control particle formation in reactive plasmas.

A vessel resembling the Gaseous Electronics Conference (GEC) reference cell is powered by two electrodes: the one at the top couples to the plasma capacitively and a pancake antenna at the bottom can heat the plasma inductively [see Fig. 1(a)]. A movable sample holder is embedded into the top electrode. It can be retracted into a load lock where it can be loaded with 2×2 cm^2 sized flat silicon substrates. The gas pressure is controlled by a butterfly valve that connects the vessel with the pumping cabinet. Up to three gases can be fed into the reactor by mass flow controllers via a ring shaped gas shower. The reactor is equipped with several diagnostics such as a spectroscopic *in situ* ellipsometer, a Langmuir probe system, a mass spectrometer, a photodiode, and a high speed intensified charge coupled device (ICCD)

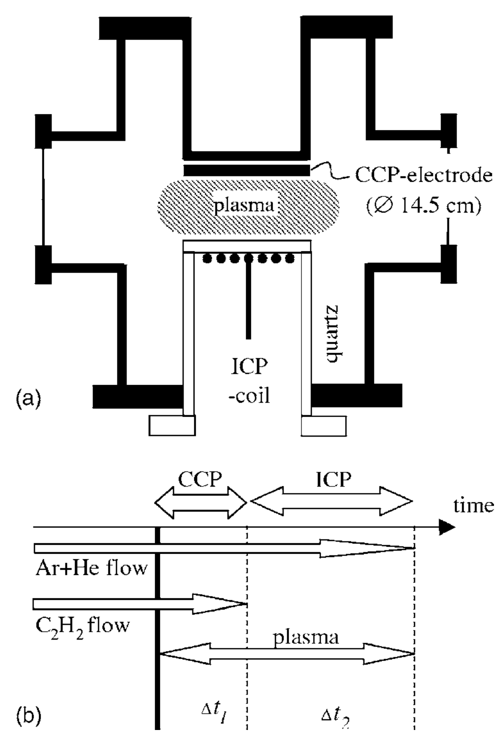

FIG. 1. (a) Sketch of the GEC-like ICP chamber. (b) Timing of the particle generation.

[a]Electronic mail: martin.schulze@rub.de

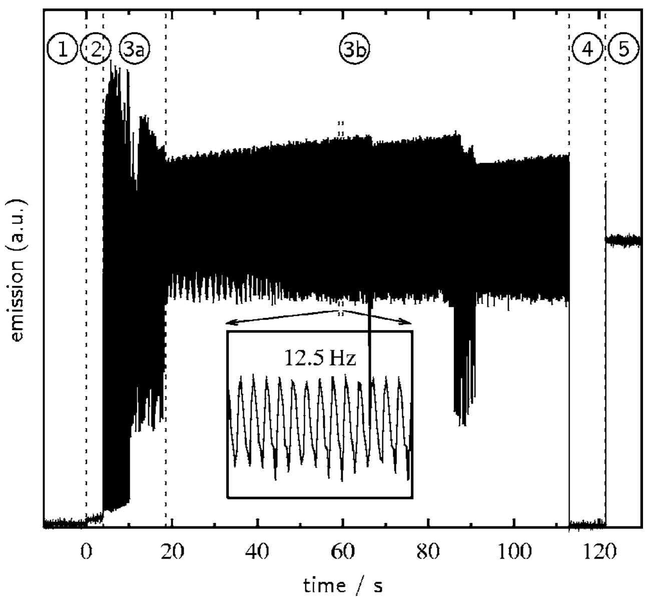

FIG. 2. Optical plasma emission during a sequence of preparation (1), acetylene injection (2), oscillations (3), plasma interruption (4), and stable discharge (5). The discharge is powered by the capacitive electrode during (2) and by the inductive coil during (3) and (5).

camera with an acousto-optical wavelength filter.

The experiments are carried out as follows [see Fig. 1(b)]: first (1) a flow of argon and helium as buffer gas is set to 4 SCCM (SCCM denotes cubic centimeter per minute at STP) (argon) and 15 SCCM (helium) at a pressure of 4 Pa. Acetylene is added at a flow rate $\phi_{C_2H_2}$; next (2), a capacitive discharge at a forward power of 70 W is ignited for a time period Δt_1 to induce particle formation; then (3) the acetylene flow is switched off and the antenna is used to sustain the plasma in the inductive mode at 100 W forward power for a time period $\Delta t_2 = 120$ s. The particles generated from acetylene in (2) stay confined in the discharge during phase (3); afterwards (4) the plasma is switched off and the particles are collected on the silicon substrate for *ex situ* analysis with an atomic force microscope (AFM) and a scanning electron microscope (SEM).

The overall optical emission of the plasma is measured by a photodiode. The time evolution for an experiment with $\phi_{C_2H_2} = 4$ SCCM and $\Delta t_1 = 4$ s is shown in Fig. 2. During the capacitive plasma phase (2), the light emission is low compared to the inductive phase (3) due to the much lower electron density. When powering the inductive antenna, the plasma oscillations during phase (3) become clearly visible. After interrupting the plasma (4) for a few seconds, the plasma is switched on again and the emission remains stable [phase (5) in Fig. 2] from then on.

The principle mechanism driving the observed plasma instability has been discussed in Ref. 7: during the injection phase (2), particles are formed from acetylene. When the inductive antenna is properly powered, the plasma impedance is at the edge of the transition between capacitive and inductive modes. Fluctuations in the spatial particle distribution cause strong variations in the heating efficiency, leading to an oscillation between capacitive and inductive modes. Consequently, a strong, chaotic modulation of the plasma emission is observed [phase (3a) in Fig. 2]. The situation is comparable to an electron attachment instability with characteristic frequencies of $10^2 - 10^4$ Hz that has been observed in electronegative discharges.[8] However, unlike this attachment instability where the electronegative species experience a periodic transition from neutral state to negative ion to neutral to positive ion, the charge state of the particles in this experiment depends predominantly on the particle size and remains nearly constant during the oscillations. Hence, the oscillations are not caused by charge fluctuations but by the spatial transport of the particles and the charge they carry.

After consumption of all acetylene, the growth process stops and a particle containing argon/helium discharge remains. For a discharge volume of approximately 5 l, the mean residence time of neutral species due to pumping losses is half a second. Therefore, it is reasonable to assume that the chemistry is finished within a few seconds after the supply of acetylene is stopped. The particle confinement is maintained by electrostatic force in the plasma sheaths, which keeps the negatively charged particles inside the plasma volume. The plasma is from then on purely inductive and a characteristic frequency of the oscillation up to several tens of hertz is established [phase (3b) in Fig. 2]. The nature of this oscillation will be discussed below. For the selected external parameters, particles cause an oscillation with a time period of 79 ms or a frequency of 12.5 Hz. Within the scatter of the data, this frequency stays constant for some minutes. Sporadically, a parasitic discharge in the dark room of the chamber occurs and causes more violent variations in the plasma emission (e.g., Fig. 2, 85–95 s). The reason for this could not be clarified yet. By interrupting the plasma, particles can leave the discharge [phase (4) in Fig. 2]. When the antenna is switched on again, the inductive mode is stable [period (5) in Fig. 2].

After measuring the oscillation time period during phase (3b), the particles are deposited on a silicon sample. The experiment is repeated for different injection times $\Delta t_1 = 2, 4, \ldots, 32$ s. The SEM is used to obtain high resolution images of the samples. For cases (a) 4 s, (b) 8 s, and (c) 32 s such images are shown in Fig. 3. Obviously, the isolated particles are monodisperse and have an almost perfect spherical shape. Their diameters increase with Δt_1. Apart from the isolated particles, also groups of two or more particles are visible on the images. However, a tendency to form cauliflowerlike ensembles, as reported for much larger particles in other experiments,[9] cannot be observed. Therefore, it is assumed that the particle islands on the substrate are formed during switching off the plasma. With the help of edge detection and image segmentation techniques the particle density and the diameter distribution of the isolated particles on the samples have been determined. The diameter is found to follow a Gaussian probability distribution with a standard deviation between 3 and 5 nm for all experiments. The mean diameter $\langle d \rangle$ is denoted on the images in Fig. 3.

Measurements with an AFM confirm the spherical shape of the particles. The distribution of particle heights from AFM matches also the diameter distribution from the SEM images. While the resolution of the SEM is restricted to particle diameters above $\simeq 10$ nm (the contrast of smaller particles is too weak to detect them reliably and their boundary is not sharp), the AFM would in principle allow us to measure even smaller particles. Due to problems with particle sticking to the AFM probe tip, however, it has not been possible to get reproducible images for particles < 10 nm.

Figure 4 shows the correlation between the measured oscillation time period during phase (3b) and the mean par-

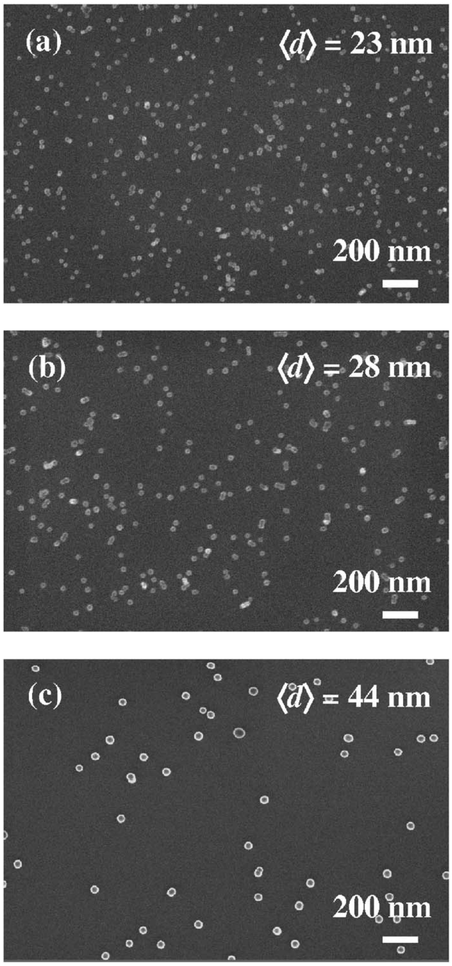

FIG. 3. SEM pictures of particles deposited onto Si samples. The injection times of C_2H_2 leading to pictures (a), (b), and (c) were 4, 8, and 32 s, respectively.

ticle diameter. To first order, a linear dependence is found to exist. But why does the oscillation frequency scale with the particle diameter?

In order to identify the physical nature of the oscillation, a Langmuir probe and a high speed ICCD camera have been used to measure the electron density temporally and spatially resolved. These data indicate that the oscillation consists of an off-centered localized void or plasmoid, which rotates around the symmetry axis of the reactor. This particle-induced rotation of a plasmoid is similar to findings in literature: for a capacitive discharge in Refs. 10 and 11 the spontaneous formation of a void in a dusty plasma has been observed, if the ion drag force becomes larger than the electrostatic force. This void rotates with frequencies in the hertz range for particles larger than 200 nm in diameter. In the inductive plasma discussed here, the ion drag force is much more intense due to the much higher electron density. As a consequence, the condition for void formation is already met for particles larger than 1 nm in diameter. It is believed that this void formation takes place in the inductive phase [period (3) in Fig. 2]. The minimum energy configuration is apparently an off-centered void which rotates around the symmetry axis of the reactor. Since the rotation of the void implies also the movement of the dusty plasma around, it is straightforward that the period of this oscillation depends also on the inertia of the particles. A correlation between oscillation period and particle diameter results. Details of the Langmuir probe measurements and the interpretation of these results will be presented elsewhere.[12]

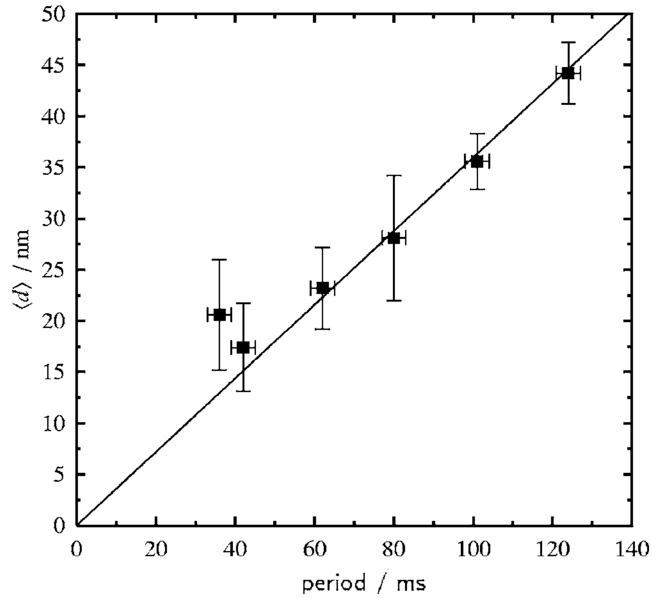

FIG. 4. Correlation between particle diameter ($\langle d\rangle$) and oscillation time period. The bars in x direction indicate the uncertainty in the time period while the bars in y direction equal the standard deviation of the particle diameter distribution. The solid line is drawn arbitrarily to indicate the first-order linearity of the dependence.

Particles have been generated by injecting acetylene in an inductive plasma from argon. This triggers an oscillation of the plasma emission. The time period of the oscillation is found to depend linearly on the mean diameter of the particles. Thereby the oscillation phenomenon can serve as monitor signal to control the size of plasma produced particles. The lower size limit of about 10 nm in the experiments discussed here is determined by the current restrictions of the imaging tools. The extension of the experiments to produce even smaller particles in a controlled manner is currently under investigation.

The authors acknowledge the support by the German Science Foundation via the SFB 591.

[1] A. Bouchoule, *Dusty Plasmas: Physics, Chemistry and Technological Impacts in Plasma Processing*, 1st ed. (Wiley, New York, 1999).
[2] C. Hollenstein, Plasma Phys. Controlled Fusion **42**, R93 (2000).
[3] V. Suendo, G. Patriarche, and P. R. i Cabarocas, Opt. Mater. **27**, 953 (2005).
[4] Z. Shen, T. Kim, U. Kortshagen, P. McCurry, and S. Campbell, J. Appl. Phys. **94**, 2277 (2003).
[5] A. F. i Morral, H. Hofmeister, and P. R. i Cabarrocas, J. Non-Cryst. Solids **299–302**, 1173 (2002).
[6] L. Boufendi, J. Gaudin, S. Huet, G. Viera, and M. Dudemaine, Appl. Phys. Lett. **79**, 4301 (2001).
[7] A. von Keudell and M. Bauer, Plasma Sources Sci. Technol. **13**, 285 (2004).
[8] P. Chabert, A. J. Lichtenberg, M. Lieberman, and A. Marakhtanov, Plasma Sources Sci. Technol. **10**, 478 (2001).
[9] I. Stefanović, E. Kovačević, J. Berndt, Y. Pendleton, and J. Winter, Plasma Phys. Controlled Fusion **47**, A179 (2005).
[10] G. Praburam and J. Goree, Phys. Plasmas **3**, 1212 (1996).
[11] D. Samsonov and J. Goree, Phys. Rev. E **59**, 1047 (1999).
[12] M. Schulze, A. von Keudell, and P. Awakowicz, Plasma Sources Sci. Technol. (submitted).